Magnetoelastic coupling across the field-induced transition of uranium mononitride

Gorbunov, D.; Nomura, T.; Zvyagin, A. A.; Henriques, M. S.; Andreev, A. V.; Skourski, Y.; Zvyagina, G. A.; Troc, R.; Zherlitsyn, S.; Wosnitza, J.;

Magnetoelastic coupling across the field-induced transition of uranium mononitride

D. I. Gorbunov,[1] T. Nomura,[1] A. A. Zvyagin,[2, 3, 4] M. S. Henriques,[5] A. V. Andreev,[5]
Y. Skourski,[1] G. A. Zvyagina,[3] R. Troć,[6] S. Zherlitsyn,[1] and J. Wosnitza[1, 7]

[1]*Hochfeld-Magnetlabor Dresden (HLD-EMFL), Helmholtz-Zentrum Dresden-Rossendorf, 01328 Dresden, Germany*
[2]*Max-Planck-Institut für Physik komplexer Systeme, 01187 Dresden, Germany*
[3]*B. I. Verkin Institute for Low Temperature Physics and Engineering of*
the National Academy of Sciences of Ukraine, Kharkiv 61103, Ukraine
[4]*V. N. Karazin Kharkiv National University, 4, Svoboda sq. Kharkiv 61022, Ukraine*
[5]*Institute of Physics, Academy of Sciences, Na Slovance 2, 182 21 Prague, Czech Republic*
[6]*W. Trzebiatowski Institute of Low Temperature and Structure Research,*
Polish Academy of Sciences, Okólna 2, 50-422 Wrocław, Poland
[7]*Institut für Festkörper- und Materialphysik, TU Dresden, 01062 Dresden, Germany*

Uranium mononitride, UN, displays a spin-flop-like transition for magnetic field applied along all principal crystallographic directions just below 60 T. Here, we report on ultrasound and magnetocaloric-effect results for UN in pulsed magnetic fields up to 65 T. The field-induced phase transition causes a discontinuous temperature decrease, indicating a larger magnetic entropy above the transition. Furthermore, we find pronounced anomalies in the acoustic properties, which signals strong spin-lattice interactions. A further anomaly observed at fields slightly above the transition is likely related to the formation of magnetic domains. A model based on the exchange-striction coupling mechanism well reproduces the strong renormalization of the acoustic properties.

I. INTRODUCTION

Uranium monopnictides, and among them the uranium mononitride, UN, attract strong attention of researchers because of two main reasons. First of all, UN is a very interesting compound from a fundamental viewpoint due to its intriguing electronic properties. Over the years, the primary focus of a large number of studies was to disclose the nature of the $5f$ electronic states, which are, most probably, responsible for the unique properties of UN. On the one hand, the $5f$ electrons are supposed to be itinerant, as suggested by studies of pressure-dependent magnetic properties, inelastic neutron scattering, and photoemission [1–3], supported by numerous band-structure calculations (see, e.g., Refs. [4–6]). On the other hand, neutron form-factor and thermal-transport properties [4, 7, 8] can be explained from the viewpoint of localized $5f$ electrons [9]. Secondly, recent studies have suggested that UN can serve as a promising fuel material for the fourth generation of nuclear reactors [10–13] raising the interest towards possible applications. This proposal is based on a combination of the high thermal conductivity [14–16], high heavy-atom density [17], and high melting point [18, 19].

UN crystallizes in a face centered cubic (fcc) NaCl-type structure [20, 21] and displays antiferromagnetic (AFM) order with moments aligned along the $\langle 100 \rangle$ axes below the Néel temperature, $T_N = 51\text{-}53$ K [7, 22–25]. The U-U distances are 3.46 Å, i.e., within the Hill limit, 3.4-3.6 Å, that marks a crossover between localized and itinerant electronic states for U-based compounds [26, 27]. Earlier studies of the magnetic properties of UN suggest that the $5f$ electrons are predominantly itinerant. Namely, the ordered moment per U atom, $M_U = 0.75$ μ_B [7], and the effective moment, $M_{eff} \approx 2.7$ μ_B [4, 23], are lower than 3.58 and 3.62 μ_B expected for the $5f^2$ and

$5f^3$ configurations, respectively. In addition, the equally large reduction rates of M_U and T_N under pressure were taken as evidence that UN is a band antiferromagnet [1]. However, the large magnetic entropy and magnetic field-induced spin-flop-like phase transition, observed recently in UN [28, 29] support the picture of rather localized magnetic moments.

For the $5f$ electrons in UN, a number of calculations suggest a mixed covalent (U $5f$ - N $2p$ hybridization) and metallic (U $5f$ - U $5f$ and U $5f$ - U $6d$ hybridization) bonding character [4, 30–34]. Photoelectron spectroscopy studies on single crystals and thin films show that the density of states at the Fermi level is dominated by the U $5f$ states [3, 4, 35–38]. However, a number of experiments point out that part of the $5f$ states are below the Fermi energy [4, 36–38]. This strongly suggests the dual nature of the $5f$ electronic states in UN as postulated in Ref. [39]. Such a dual nature of the U $5f$ electrons in uranium mononitride was also derived from the results of some state-of-the-art calculations based on a combination of density-functional theory with dynamical mean-field theory, which reproduced experimental photoemission data better than previous standard approaches, see, e.g., Ref. [11].

Earlier high-field magnetization measurements up to 40 T did not show any anomaly [40]. However, recent experiments up to higher fields revealed a spin-flop-like transition just below 60 T [28, 29]. This magnetization jump likely originates from a reorientation of part of the U magnetic moments along the applied field. The transition is accompanied by a large negative longitudinal magnetostriction, $\epsilon_{100} \approx -5 \times 10^{-5}$ and $\epsilon_{110} \approx -15 \times 10^{-5}$, for field applied along the [100] and [110] axes, respectively [29]. The large length changes of the sample suggest strong spin-lattice coupling. The ultrasound technique is known to be a highly sensitive probe of magne-

toelastic interactions [41] and has the potential to provide crucial information about this field-induced transition.

Indeed, we find pronounced anomalies in the sound velocity and sound attenuation at the field-induced transition for field applied along the principal crystallographic directions of UN. We also observe further features above the transition which are likely related to the formation of high-field magnetic domains. A model based on the exchange-striction coupling well reproduces the large renormalization of the acoustic properties.

II. EXPERIMENTAL DETAILS

UN single crystals were prepared as described in Ref. [28]. The crystal structure was checked using single-crystal x-ray diffraction. The diffracted intensities were collected at ambient temperature using a four-circle diffractometer (Gemini of Agilent) equipped with a Mo tube and an Atlas CCD detector. The CrysAlis PRO [42] program was used to index the lattice, refine the unit cell, reduce the data, and perform the absorption correction. The structure refinements were carried out using the program JANA2006 [43]. The crystal structure was solved in the space group Fm-$3m$ (type NaCl) and the final refined lattice constant was found to be $a = 4.887(7)$ Å. Backscattered Laue diffraction was used to check the single-crystalline state and to orient the crystals for ultrasound, magnetocaloric-effect, and magnetization measurements.

The field and temperature dependences of the relative sound-velocity, $\Delta v/v$, and sound-attenuation, $\Delta\alpha$, changes were measured using a phase-sensitive pulse-echo technique [41, 44] in zero and in pulsed magnetic fields up to 65 T. A pair of piezoelectric transducers were glued to opposite surfaces of the sample in order to excite and detect acoustic waves. We measured the longitudinal, C_{11} ($\boldsymbol{k} \parallel \boldsymbol{u} \parallel [100]$), $C_{L[110]} = \frac{1}{2}(C_{11} + C_{12} + 2C_{44})$ ($\boldsymbol{k} \parallel \boldsymbol{u} \parallel [110]$), and transverse, C_{44} ($\boldsymbol{k} \parallel [110], \boldsymbol{u} \parallel [100]$), elastic moduli. Here, $\boldsymbol{k}$ and $\boldsymbol{u}$ are the wavevector and polarization of the acoustic waves, respectively. The room-temperature absolute values of sound velocity for these acoustic modes, $v_{11} = [5390 \pm 200]$ m/s, $v_{L[110]} = [4780 \pm 200]$ m/s, and $v_{44} = [2270 \pm 100]$ m/s, are in good agreement with literature [45–47] when estimated using the relation $v = \sqrt{C/\rho}$, where $\rho = 14.32 \times 10^3$ kg/m^3 is the mass density of UN [17, 45, 46]. The ultrasound frequencies varied between 109 and 130 MHz in our experiments.

The adiabatic temperature change (magnetocaloric effect, MCE) of the sample during field pulses was measured using a RuO$_2$ thermometer (900 Ω, $0.6 \times 0.3 \times 0.1$ mm^3) [48, 49]. The thermometer was sandwiched between two single crystals placed in a vacuum environment ensuring adiabatic condition. The resistance of the thermometer was measured with a standard ac four-probe method using a numerical lock-in technique at a frequency of 50 kHz.
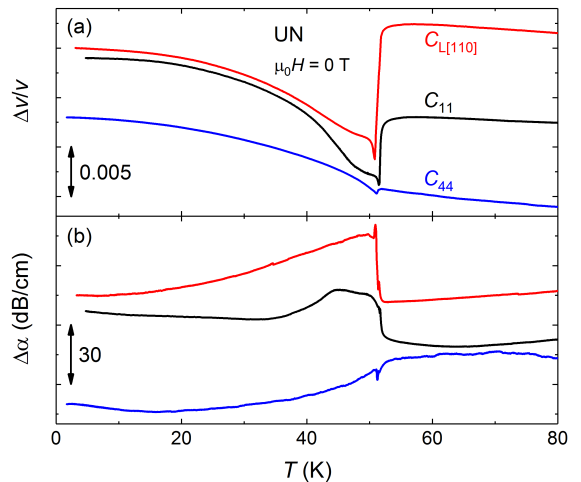

FIG. 1: Temperature dependences of (a) the relative sound-velocity changes, $\Delta v/v$, and (b) the sound attenuation, $\Delta\alpha$, of UN in zero magnetic field. The curves are vertically offset for clarity.

III. RESULTS

The crystal lattice of uranium mononitride is strongly coupled to the magnetic degrees of freedom as seen from a pronounced jump of $\Delta v/v$ at $T_{\mathrm{N}} = 51$ K [Fig. 1(a)]. This result is in good agreement with previous elastic-modulus measurements [46, 47]. We recall that UN transforms from the cubic paramagnetic state into the tetragonal AFM state, albeit with a very small tetragonal distortion, $c/a = 0.99935$ [50]. This tiny lattice deformation is unlikely to lead to the large changes in $\Delta v/v$ observed in experiment. We, therefore, assume that the jump-like anomaly of $\Delta v/v$ has a magnetic origin. The lattice hardening below T_{N} evidently relates to the antiferromagnetic order.

The phase transition into the AFM state also leads to significant anomalies in the sound attenuation [Fig. 1(b)]. As the temperature decreases, $\Delta\alpha$ grows substantially at T_{N} for longitudinal acoustic waves. While a single sharp anomaly is observed for the acoustic mode $C_{L[110]}$ at T_{N}, an additional kink emerges for C_{11} at 44 K. Note that the thermal-expansion coefficient shows an anomaly at about the same temperature as well [29]. The origin of this anomaly is not clear yet. For the transverse acoustic waves (C_{44}), $\Delta\alpha$ exhibits a minimum at T_{N}.

The observed strong spin-strain coupling in uranium mononitride suggests that anomalies in ultrasound can be expected in applied field as well. Below, we concentrate on the magnetic and elastic properties of UN in high magnetic fields.

At 2 K, the magnetization, M, displays a spin-flop-like transition at 57.8, 57.3, and 53 T for field applied along the [100], [110], and [111] axes, respectively [Figs. 2(a), (b), and (c)]. The transitions are accompanied by a pronounced softening for both, longitudinal and transverse,
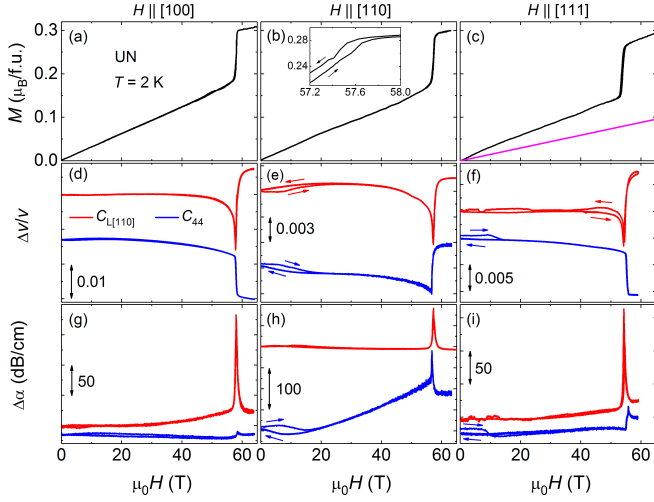
FIG. 2: Magnetization, M, relative sound-velocity changes, $\Delta v/v$, and sound attenuation, $\Delta\alpha$, for field applied along the (a, d, g) [100], (b, e, h) [110], and (c, f, i) [111] axes of UN at 2 K. The M data were taken from Ref. [28]. The $\Delta v/v$ and $\Delta\alpha$ curves are vertically offset for clarity. The inset in panel (b) shows an enlarged view of M just above the spin flop. The magenta curve in panel (c) shows the estimated Pauli magnetization.

acoustic modes [Figs. 2(d), (e), and (f)]. We observe the largest effect, $\approx 1\%$, when the field is applied along the [100] direction. The sound attenuation shows large peaks at the transitions, specifically for the longitudinal acoustic waves [Figs. 2(g), (h), and (i)]. For $\boldsymbol{H} \parallel$ [100], $\Delta\alpha$ even exceeds 150 dB/cm.

A broad hysteresis was also detected below approximately 15 T when the field was applied along the [110] and [111] axes [Figs. 2(e), (f), (h), and (i)]. This correlates with magnetostriction results and likely originates from a rearrangement of magnetic domains [29].

An earlier high-field study showed that the critical field and the magnetization jump at the field-induced transition decreased monotonously upon approaching T_{N} [28]. Upon increasing temperature towards T_{N}, our pulsed-field ultrasound experiments reveal unexpected features. For longitudinal acoustic waves, $\Delta v/v(H)$ shows the largest softening followed by a jump of several percent at temperatures between 25 and 40 K [Figs. 3(a), (b), and (c)]. In the same temperature range, the large peak in $\Delta\alpha$ changes to a much smaller anomaly for $\boldsymbol{H} \parallel$ [100] and $\boldsymbol{H} \parallel$ [110] [Figs. 3(d) and (e)]. By contrast, for $\boldsymbol{H} \parallel$ [111], $\Delta\alpha$ displays anomalies of comparable magnitude at all temperatures below T_{N} [Fig. 3(f)].

Above 2 K, the field dependences of the sound velocity show an additional step-like hardening just above the spin flop for $\boldsymbol{H} \parallel$ [100] and $\boldsymbol{H} \parallel$ [110] [Figs. 3(a) and (b)]. Notice that the magnetization exhibits a tiny anomaly just above the spin-flop transition, too [inset in Fig. 2(b)]. With increasing temperature, the minimum in $\Delta v/v$ becomes small in comparison with the step-like anomaly. The sound attenuation also shows features at the same
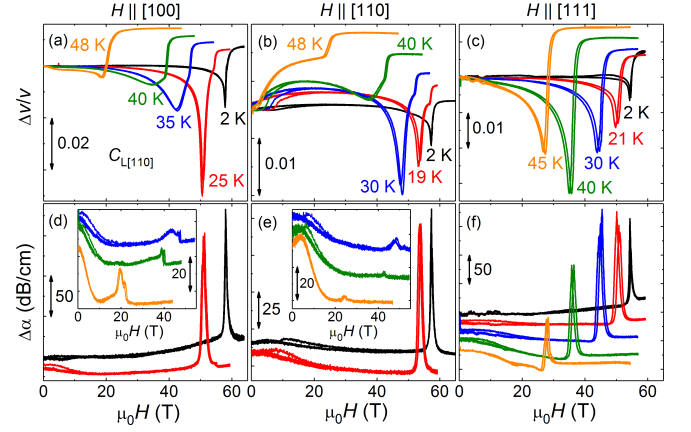

FIG. 3: Relative sound-velocity changes, $\Delta v/v$, and sound attenuation, $\Delta\alpha$, for the acoustic mode $C_{\mathrm{L}[110]}$ for field applied along the (a, d) [100], (b, e) [110], and (c, f) [111] axes of UN. The insets in panels (d) and (e) show $\Delta\alpha$ at elevated temperatures. The $\Delta\alpha$ curves are vertically offset for clarity.
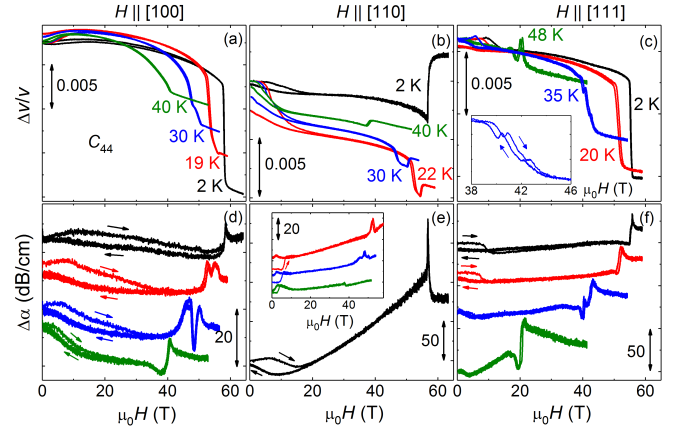

FIG. 4: Relative sound-velocity changes, $\Delta v/v$, and sound attenuation, $\Delta\alpha$, for the acoustic mode C_{44} for field applied along the (a, d) [100], (b, e) [110], and (c, f) [111] axes of UN. The inset in panel (c) shows an enlarged view of $\Delta v/v$ at 35 K. The inset in panel (e) shows $\Delta\alpha$ at elevated temperatures. The $\Delta\alpha$ curves are vertically offset for clarity.

fields as the anomalies seen in $\Delta v/v$ [Figs. 3(d) and (e)].

The double anomalies emerge in $\Delta v/v(H)$ above 2 K for transverse acoustic waves as well. These anomalies are evident in $\Delta v/v$ and $\Delta\alpha$ for $\boldsymbol{H} \parallel$ [100] and $\boldsymbol{H} \parallel$ [110] [Figs. 4(a), (b), (d), and (e)]. For $\boldsymbol{H} \parallel$ [111], even a more complex fine structure can be resolved in the vicinity of the spin flop, e.g., for the field sweep at 35 K [Figs. 4(c) and (f)].

Our high-field $\Delta v/v$ and $\Delta\alpha$ data allow us to estimate the characteristic relaxation time, τ, related to the spin flop. We use the Landau-Khalatnikov relation,

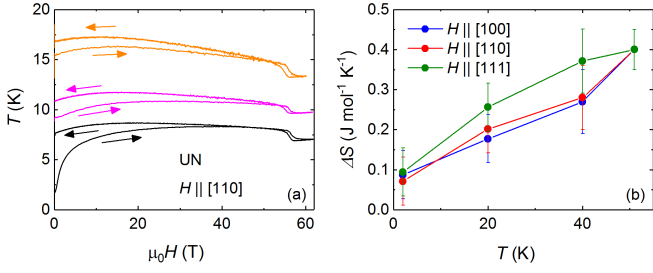$$\tau = \frac{v}{\omega^2}\frac{\Delta\alpha}{\left(-\frac{\Delta v}{v}\right)}, \qquad (1)$$

FIG. 5: (a) MCE for field applied along the [110] axis of UN and (b) entropy increase, ΔS, at the spin flop according to the Eq. (2) using magnetization data from Ref. [28].

where ω is the angular frequency [41]. Strictly speaking, Eq. (1) is valid for $\omega\tau \ll 1$. However, it still gives an approximate value of τ unless $\omega\tau \gg 1$ [51].

Our estimates show that for the acoustic mode $C_{L[110]}$, τ decreases from $\sim 10^{-9}$ s ($\omega\tau \approx 3$) to $\sim 10^{-10}$ s ($\omega\tau \approx 0.3$) in the vicinity of 30 K with temperature and field applied along the [100] and [110] directions. This is the temperature region where the large peak in $\Delta\alpha$ changes to much smaller anomalies [see Figs. 3(d) and (e)]. The relaxation time associated with the additional anomaly that emerges at elevated temperatures is $\sim 10^{-10}$ s ($\omega\tau \approx 0.3$) for both field directions. For field applied along the [111] axis, the peak in $\Delta\alpha$ at the spin-flop transition decreases gradually with temperature, and the corresponding relaxation time also changes gradually from $\sim 10^{-8}$ s ($\omega\tau \approx 8$) at low temperatures to $\sim 10^{-9}$ s ($\omega\tau \approx 0.8$) at higher temperatures.

For the acoustic mode C_{44}, we could estimate the relaxation time at the anomaly observed in $\Delta\alpha$ below 30 K. For $\boldsymbol{H} \parallel$ [100], τ increases from $\sim 10^{-10}$ s ($\omega\tau \approx 0.2$) at 2 K to $\sim 10^{-9}$ s ($\omega\tau \approx 2$) at 30 K. For $\boldsymbol{H} \parallel$ [110] and $\boldsymbol{H} \parallel$ [111], the relaxation time is almost constant, $\tau \sim 10^{-9}$ s ($\omega\tau \approx 1$), between 2 and 30 K.

For both acoustic modes $C_{L[110]}$ and C_{44}, the estimated relaxation time is relatively long and characteristic of spin fluctuations.

Figure 5(a) shows the temperature of the sample as a function of field applied along the [110] axis under adiabatic conditions. Initially, the temperature increases presumably due to eddy currents and, possibly, domain reorientation, and then levels off. The spin flop causes the temperature to decrease discontinuously by 1 K, indicating that the magnetic entropy above the transition is larger. A small hysteresis is observed here as appropriate for a first-order phase transition.

The change of the entropy, ΔS, associated with the phase transition can be estimated using the Clausius-Clapeyron relation [52],

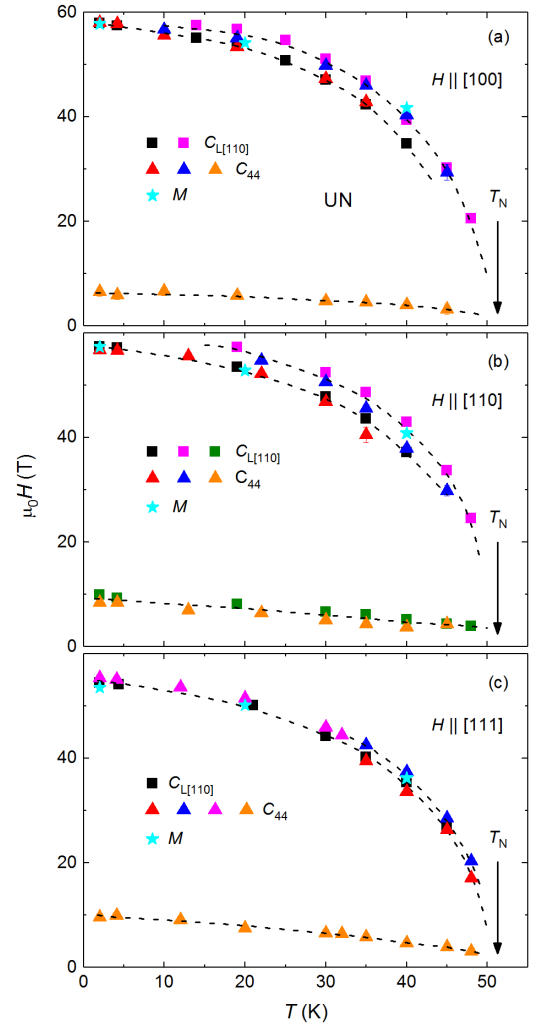$$\Delta S = -\Delta M \left(\frac{dH_c}{dT_c} \right). \qquad (2)$$

FIG. 6: Magnetic phase diagrams of UN for field applied along the (a) [100], (b) [110], and (c) [111] directions. Lines are guides to the eye. The error bars are of the order of symbol size.

Here, the slope of the phase boundary, dH_c/dT_c, is obtained from the phase diagram shown in Fig. 6, and the magnetization jump, ΔM, is taken from a previous high-field magnetization study [28]. ΔS at zero field is obtained using the specific-heat data around T_N [29]. The associated entropy change is 0.4 J mol^{-1} K^{-1} at 51 K and decreases to about 0.15 J mol^{-1} K^{-1} at 10 K [Fig. 5(b)] as a result of the AFM ordering.

The H-T phase diagram of UN (Fig. 6) resembles those reported in Refs. [28, 29]. The low-field line below about 10 T likely reflects domain reorientation. A spin flop occurs just below 60 T. Previous magnetization and magnetostriction experiments showed single broad anomalies due to the spin flop at elevated temperatures, whereas our ultrasound measurements revealed additional features related to another field-induced transition. These features are presented as two lines in the high-field part of the phase diagram.

IV. DISCUSSION

The dual nature of the $5f$ electrons was considered in the so-called dual-nature model [53–57] with competing localized and delocalized $5f$ electrons for both exact and perturbative theoretical approaches. Localized states of U ions lying near the Fermi energy can hybridize with conduction electrons and, thus, experience a weak dispersion (narrow bands), enhancing the density of states at the Fermi surface. On the other hand, only part of the $5f$ electrons of the U ions may become itinerant, while the rest remains localized in the vicinity of the Fermi surface. In fact, our results support the latter picture. Such a dual model explains the coexistence of the magnetic and superconducting properties of several U compounds.

However, band-structure calculations cannot explain the features of the magnetic and magnetoelastic characteristics reported in this paper. Comparing the Pauli magnetization with our data, the dual nature of the $5f$ electrons of U can be seen, for example, in Fig. 2(c). Here, we present the calculated contribution of the itinerant electrons to the low-temperature magnetization of UN. The magnetic susceptibility of the conduction electrons (assumed to be noninteracting in our estimates) was obtained from the value of the Sommerfeld coefficient, 0.045 J mol^{-1} K^{-2}, for the linear in T contribution to the specific heat [28]. Evidently, the contribution from the conduction electrons is essential in UN, confirming the dual nature of the $5f$ electrons. On the other hand, itinerant electrons themselves cannot explain the observed spin-flop-like phase transition, which is related to the localized magnetic moments (see below).

The renormalization of the sound velocities and attenuation in magnetic systems is caused mostly by two factors [41]. First, sound waves change the ligand (nonmagnetic ions surrounding the magnetic ones) positions, and, therefore, the crystalline electric field (CEF) of the ligands is affected. Due to the strong spin-orbit interaction, the CEF yields changes of the single-ion magnetic anisotropy of the magnetic ions. It also changes the effective g-factors of the magnetic ions. Hence, due to magnetoelastic coupling, sound waves can change slightly the direction of the magnetic anisotropy, and vice versa, the magnetic anisotropy modifies the acoustic properties, such as the sound velocity and attenuation. This effect has a relativistic nature and the interaction between the sound wave and the magnetic material properties exists at any temperature lower than the characteristic energy of the single-ion magnetic anisotropy.

Secondly, sound waves change the positions of magnetic ions and the positions of nonmagnetic ions involved in the indirect exchange coupling (superexchange [58]). In this case, sound waves renormalize the effective exchange interactions between magnetic ions. Typically, this effect is more pronounced than strain-single-ion coupling since the interionic exchange interactions determine predominantly magnetic phase transitions in ordered magnets. Hence, here we consider such an exchange-

striction mechanism to describe our experimental observations.

According to Ref. [59], the exchange-striction coupling in magnetic systems yields a renormalization of the velocity of the sound wave, proportional to some spin-spin correlation functions. These correlation functions can be approximated by a combination of the magnetization and the magnetic susceptibility of the system. References [60–62] present good agreements between experiments and theory for many magnetic systems even if only the homogeneous part of the magnetic susceptibility is taken into account. The renormalization of the sound velocity, v, due to the exchange-striction coupling in the general case can be written as

$$\frac{\Delta v}{v} \approx -\frac{v}{\rho V \omega^2 \mu^4} \times$$
$$\times \left[|g(0)|^2 (2M^2\chi + T\chi^2) + h(0)\mu^2(M^2 + T\chi) \right], \quad (3)$$

where V is the volume of the crystal, μ is the effective magneton per magnetic ion, and χ is the magnetic susceptibility. The magnetoelastic coefficients are

$$h = \sum_j e^{i\mathbf{q}\mathbf{R}_{ji}} \left[1 - \cos(\mathbf{k}\mathbf{R}_{ji}) \right] (\mathbf{u_k} \cdot \mathbf{u_{-k}}) \frac{\partial^2 J_{ij}^{\beta,\beta'}}{\partial \mathbf{R}_i \partial \mathbf{R}_j}),$$

$$g = \sum_j e^{i\mathbf{q}\mathbf{R}_{ji}} \left(e^{i\mathbf{k}\mathbf{R}_{ji}} - 1 \right) \mathbf{u_k} \frac{\partial J_{ij}^{\beta,\beta'}}{\partial \mathbf{R}_i} \quad (4)$$

(taken at $\mathbf{q} = 0$), where $\mathbf{R}_{ji} = \mathbf{R}_j - \mathbf{R}_i$, $\mathbf{R}_j$ is the position vector of the j-th site of the magnetic ion, and $J_{ij}^{\beta,\beta'}$ ($\beta,\beta' = x,y,z$) are the exchange couplings between magnetic ions on the i-th and j-th site. Similar results can be obtained for the sound attenuation,

$$\Delta\alpha \approx \frac{\gamma}{\rho V v \mu^4 (\omega^2 + \gamma^2)} \times$$
$$\times \left[|g(0)|^2 (2M^2\chi + T\chi^2) + h(0)\mu^2(M^2 + T\chi) \right], \quad (5)$$

where γ is the effective relaxation rate. The results of calculations, which use the exchange-striction model, are presented in Figs. 7 and 8 for the renormalization of the sound velocity and attenuation in UN at 2 and 20 K, respectively. Excellent qualitative agreement of the results with the data of our experiments, presented in Figs. 2-4, is found. The difference between the longitudinal $C_{L[100]}$ and transverse mode C_{44} is determined by the relatively large contribution from the magnetoelastic coefficient g [Eq. (4)] for the longitudinal modes, although h dominates for the transverse modes.

The exchange-striction model correctly reproduces the main acoustic features at the critical field. Calculations for higher temperatures show a broadening of the anomaly with a transformation from first to second-order phase transition at elevated temperatures. This is a characteristic feature of Ising magnetic systems (with the magnetic-anisotropy energy being of the same order as
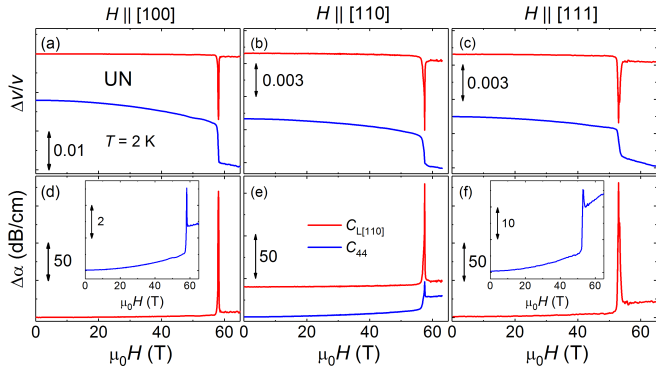
FIG. 7: Calculated relative sound-velocity, $\Delta v/v$, and sound attenuation, $\Delta\alpha$, changes for the acoustic modes $C_{\mathrm{L[110]}}$ and C_{44} and field applied along the (a, d) [100], (b, e) [110], and (c, f) [111] axes of UN at 2 K. The insets in panels (d) and (f) show $\Delta\alpha$ for C_{44}. The $\Delta v/v$ and $\Delta\alpha$ curves are vertically offset for clarity.
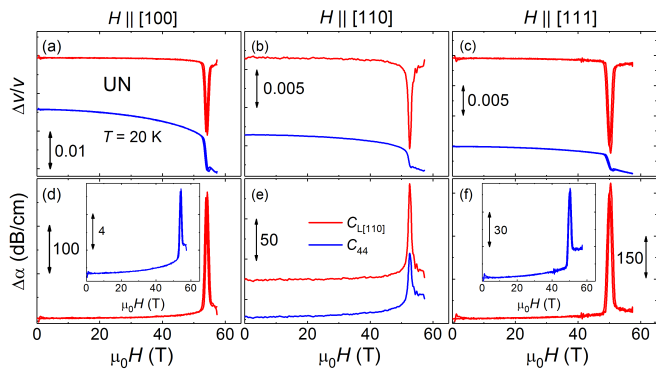

FIG. 8: Calculated relative sound-velocity, $\Delta v/v$, and sound attenuation, $\Delta\alpha$, changes for the acoustic modes $C_{\mathrm{L[110]}}$ and C_{44} and field applied along the (a, d) [100], (b, e) [110], and (c, f) [111] axes of UN at 20 K. The insets in panels (d) and (f) show $\Delta\alpha$ for C_{44}. The $\Delta v/v$ and $\Delta\alpha$ curves are vertically offset for clarity.

the exchange interactions) with metamagnetic-like phase transitions [63].

For $T \sim T_{\mathrm{N}}$ or higher, our calculations do not reveal any anomalies in the magneto-acoustic properties (not shown): They reproduce the monotonic behavior observed in experiments. In addition, we see that the smaller features at about 2-3 T and above the spin-flop phase transition are also reproduced (Fig. 8). The missing fine structure above the spin-flop transition for the 2 K data might be masked by the strong anomaly at the spin-flop transition itself. On the other hand, as mentioned above, a structural phase transition occurs at about T_{N} [50]. The related structural distortions can be the reason for the enhancement of these features at relatively high temperatures (below the Néel temperature). The discrepancies between the calculated and experimen-

tal results (e.g., the larger changes in the acoustic properties below the spin-flop transition, cf. Figs. 2 and 7) are probably related to the dropped contribution of the inhomogeneous magnetic susceptibility in our calculations.

Now, let us discuss the nature of the observed fine structure in the magneto-acoustic properties. Two possible scenarios can be considered. First, in the Ising layered model used in Ref. [28], the transformation from the AFM to the spin-flip phase might happen via two phase transitions: AFM $\to f12 \to f6$ in notations of Ref. [28].

Another possibility would be an intermediate state (see, e.g, Ref. [64] and references therein). For example, similar features have been observed for the sound velocity in $PrFe_3(BO_3)_4$ above the spin-flop transition [65]. The intermediate state for magnetic fields larger than the critical field of the spin-flop or metamagnetic phase transition [66] is related to the instability of this phase with respect to the onset of magnetic domains. Magnetic domains with magnetic moments directed along [100] and equivalent [010] and [001], having similar energies, open the possibility for domain formation. In a magnetic sample the domain structure appears because the magnetization tends to be parallel to the surface, while in the bulk of the sample the "easy-axis" magnetic anisotropy determines the direction of the magnetization. Obviously, in antiferromagnets a nonzero magnetization exists only for fields larger than the critical field of the spin-flop transition.

In summary, we have performed ultrasound and magnetocaloric-effect measurements of uranium mononitride. The MCE data reveal a discontinuous decrease of the temperature at the spin-flop-like transition, evidencing a larger magnetic entropy above the transition. We have also observed a large renormalization of the sound velocity and sound attenuation of longitudinal and transverse acoustic waves. The pronounced anomalies in $\Delta v/v$ and $\Delta\alpha$ can be explained using a model based on the exchange-striction coupling mechanism. Just above the field-induced transition, our measurements have revealed additional features that are likely related to the formation of magnetic domains. Our results obtained in high magnetic fields confirm the dual nature of the $5f$ electrons in uranium mononitride.

[1] J. M. Fournier, J. Beille, A. Boeuf, C. Vettier, and A. Wedgwood, Physica B **102**, 282 (1980).

[2] T. M. Holden, W. J. L. Buyers, E. C. Swensson, and G. H. Lander, Phys. Rev. B **30**, 114 (1984).

[3] S. Fujimori, T. Ohkochi, T. Okane, Y. Saitoh, A. Fujimori, H. Yamagami, Y. Haga, E. Yamamoto, and Y. Onuki, Phys. Rev. B **86**, 235108 (2012).

[4] M. Samsel-Czekała, E. Talik, P. de V. Du Plessis, R. Troć, H. Misiorek, and C. Sułkowski, Phys. Rev. B **76**, 144426 (2007).

[5] R. Atta-Fynn and A. K. Ray, Phys. Rev. B **76**, 115101 (2007).

[6] D. Gryaznov, E. Heifets, and E. Kotomin, Phys. Chem. Chem. Phys. **14**, 4482 (2012).

[7] N. A. Curry, Proc. Phys. Soc. London **86**, 1193 (1965).

[8] R. H. Lemmer, and J. E. Lowther, J. Phys. C **11**, 1145 (1978).

[9] J. Grunzweig-Genossar, M. Kuznietz, and F. Friedman, Phys. Rev. **173**, 562 (1968).

[10] R. K. Thomson, T. Cantat, B. L. Scott, D. E. Morris, E. R. Batista, and J. L. Kiplinger, Nat. Chem. **2**, 723 (2010).

[11] Q. Yin, A. Kutepov, K. Haule, G. Kotliar, S. Y. Savrasov, and W. E. Pickett, Phys. Rev. B **84**, 195111 (2011).

[12] T. Schuler, D. A. Lopes, A. Claisse, and P. Olsson, Phys. Rev. B **95**, 094117 (2017).

[13] G. Youinou and R. Sonat Sen, Nucl. Technol. **188**, 123 (2014).

[14] L. G. Radosevich and W. S. Williams, J. Am. Ceram. Soc. **52**, 514 (1969).

[15] S. B. Ross, M. S. El-Genk, and R. B. Matthews, J. Nucl. Mater. **151**, 313 (1988).

[16] V. I. Vybyvanets, M. L. Taubin, E. S. Solntseva, I. E. Galev, V. G. Baranov, A. V. Tenishev, and O. V. Khomyakov, At. Energ. **117**, 257 (2014).

[17] S. L. Hayes, J. K. Thomas, and K. L. Peddicord, J. Nucl. Mater. **171**, 262 (1990).

[18] W. M. Olson and R. N. R. Mulford, J. Phys. Chem. **67**, 952 (1963).

[19] H. Tagawa, J. Nucl. Mater. **51**, 78 (1974).

[20] R. E. Rundle, N. C. Baenziger, A. S. Wilson, and R. A. McDonald, J. Am. Chem. Soc. **70**, 99 (1948).

[21] M. H. Mueller and H. W. Knott, Acta Cryst. **11**, 751 (1958).

[22] T. Ohmichi, S. Nasu, and T. Kikuchi, J. Nucl Sci. Technol. **9**, 11 (1972).

[23] C. F. Van Doorn and P. de V. du Plessis, J. Low. Temp. Phys. **28**, 391 (1977).

[24] J. Rossat-Mignod, P. Burlet, S. Quezel, and O. Vogt, Physica B & C **102**, 237 (1980).

[25] K. H. Münch, A. Kratzer, G. M. Kalvius, L. Asch, F. J. Litterst, and K. Richter, Hyperfine Interact. **78**, 435 (1993).

[26] H. Hill, *Plutonium*, edited by W. N. Miner (AIME, New York, 1970) 2.

[27] V. Sechovský and L. Havela, in *Handbook of Magnetic Materials*, edited by K. H. J. Buschow (Elsevier, Amsterdam, 1998), Vol. 11.

[28] R. Troć, M. Samsel-Czekała, A. Pikul, A. V. Andreev, D. I. Gorbunov, Y. Skourski, and J. Sznajd, Phys. Rev. B **94**, 224415 (2016).

[29] K. Shrestha, D. Antonio, M. Jaime, N. Harrison, D. S. Mast, D. Safarik, T. Durakiewicz, J.-C. Griveau, and K. Gofryk, Sci. Rep. **7**, 6642 (2017).

[30] P. Weinberger, C. P. Mallet, R. Podloucky, and A. Neckel, J. Phys. C **13**, 173 (1980).

[31] M. S. S. Brooks and P. J. Kelly, Phys. Rev. Lett. **51**, 1708 (1983).

[32] M. S. S. Brooks, J. Phys. F: Met. Phys. **14**, 639 (1984).

[33] M. S. S. Brooks, J. Phys. F: Met. Phys. **14**, 857 (1984).

[34] M. S. S. Brooks, Physica B **130**, 6 (1985).

[35] P. R. Norton, R. L. Tapping, D. K. Creber, and W. J. L. Buyers, Phys. Rev. B **21**, 2572 (1980).

[36] B. Reihl, G. Hollinger, and F. J. Himpsel, Phys. Rev. B **28**, 1490 (1983).

[37] L. Black, F. Miserque, T. Gouder, L. Havela, J. Rebizant, and F. Wastin, J. Alloys Compd. **315**, 36 (2001).

[38] T. Ito, H. Kumigashira, S. Souma, T. Takahashi, and T. Suzuki, J. Magn. Magn. Mater. **226-230**, 68 (2001).

[39] R. Troć and M. Samsel-Czekała, in Programme and Proceedings of 41èmes Journées des actinides (Stará Lesná 2011), p. 19 (1O3).

[40] C. J. Schinkel and R. Troć, J. Magn. Magn. Mater. **9**, 339 (1978).

[41] B. Lüthi, *Physical Acoustics in the Solid State* (Springer, Heidelberg, 2005).

[42] CrysAlis PRO, Agilent Technologies, Version 1.171.39.46.

[43] V. Petříček, M. Dušek, and L. Palatinus, Z. Kristallogr. **229**, 345 (2014).

[44] S. Zherlitsyn, S. Yasin, J. Wosnitza, A. A. Zvyagin, A. V. Andreev, and V. Tsurkan, Low Temp. Phys. **40**, 123 (2014).

[45] M. Guinan and C. F. Cline, J. Nucl. Mater. **43**, 205 (1972).

[46] C. F. van Doorn and P. de V. du Plessis, J. Magn. Magn. Mater. **5**, 164 (1977).

[47] M. Yoshizawa, B. Lüthi, T. Goto, T. Suzuki, A. de Visser, P. Frings, and J. J. M. Franse J. Magn. Magn. Mater. **52**, 413 (1985).

[48] T. Kihara, Y. Kohama, Y. Hashimoto, S. Katsumoto, and M. Tokunaga, Rev. Sci. Instrum. **84**, 074901 (2013).

[49] T. Nomura, Y. Kohama, Y. H. Matsuda, K. Kindo, and T. C. Kobayashi, Phys. Rev. B **95**, 104420 (2017).

[50] J. A. C. Marples, C. F. Sampson, F. A. Wedgwood, and M. Kuznietz, J. Phys. C: Solid State Phys. **8**, 708 (1975).

[51] K. Kawasaki and A. Ikushima, Phys. Rev. B **1**, 3143 (1970).

[52] L. D. Landau and E. M. Lifshitz, *Statistical Physics*, 3rd ed. (Elsevier, Amsterdam, 1980), Part 1.

[53] A. A. Zvyagin, Phys. Rev. B **61**, 014503 (2001).

[54] G. Zwicknagl, A. N. Yaresko, and P. Fulde, Phys. Rev. B **65**, 081103(R) (2002).

[55] G. Zwicknagl and P. Fulde, J. Phys.: Condens. Matter **15**, S1911 (2003).

[56] A. A. Zvyagin, Eur. Phys. J. B **34**, 275 (2003).

[57] F. Pollmann and G. Zwicknagl, Phys. Rev. B **73**, 035121 (2006).

[58] J. B. Goodenough, *Magnetism and the Chemical Bond*, (Interscience, NY, 1963).

[59] M. Tachiki and S. Maekawa, Progr. Theor. Phys. **51**, 1 (1974).

[60] A. Sytcheva, O. Chiatti, J. Wosnitza, S. Zherlitsyn, A. A. Zvyagin, R. Coldea, and Z. Tylczynski, Phys. Rev. B **80**, 224414 (2009).

[61] S. Erfanifam, S. Zherlitsyn, S. Yasin, Y. Skourski, J. Wosnitza, A.A. Zvyagin, P. McClarty, R. Moessner, G. Balakrishnan, and O. A. Petrenko, Phys. Rev. B **90**, 064409 (2014).

[62] A. V. Andreev, A. A. Zvyagin, Y. Skourski, S. Yasin, and S. Zherlitsyn, Fiz. Nizk. Temp. **43**, 1575 (2017) [Low Temp. Phys. **43**, 1254 (2017)].

[63] K. Motizuki, J. Phys. Soc. Jpn. **14**, 759 (1959).

[64] V. V. Eremenko and V. A. Sirenko, *Magnetic and Magnetoelastic Properties of Antiferromagnets and superconductors*, (Cambridge Sceientific Publishers, Cambridge, 2008).

[65] G. A. Zvyagina, K. R. Zhekov, A. A. Zvyagin, I. V. Bilych, L. N. Bezmaternyh, and I. A. Gudim, Fiz. Nizk. Temp. **34**, 376 (2010) [Low Temp. Phys. **34**, 296 (2010)].

[66] It is usually accepted that for the metamagnetic type of a field-induced first-order phase transition the energy of the "easy-axis" magnetic anisotropy is of the same order as the exchange energy, such as in Ising antiferromagnets, while for the spin-flop type the energy of the anisotropy is much smaller than the exchange energy.